Electronic Supplementary Material (ESI) for Journal of Materials Chemistry A.

Supporting Information

Impact of Controlling the Crystallinity on Bifunctional Electrocatalytic Performances toward Methanol Oxidation and Oxygen Reduction in Binary Pd-Cr Solid Solution

Dasol Jin, Youngmi Lee, In Young Kim, Chongmok Lee* and Myung Hwa Kim*

Department of Chemistry & Nanoscience, Ewha Womans University, Seoul 03760, Korea

*Correspondence: myungkim@ewha.ac.kr (M.H.K.), cmlee@ewha.ac.kr (C.L.)

Supplementary Figures and Table

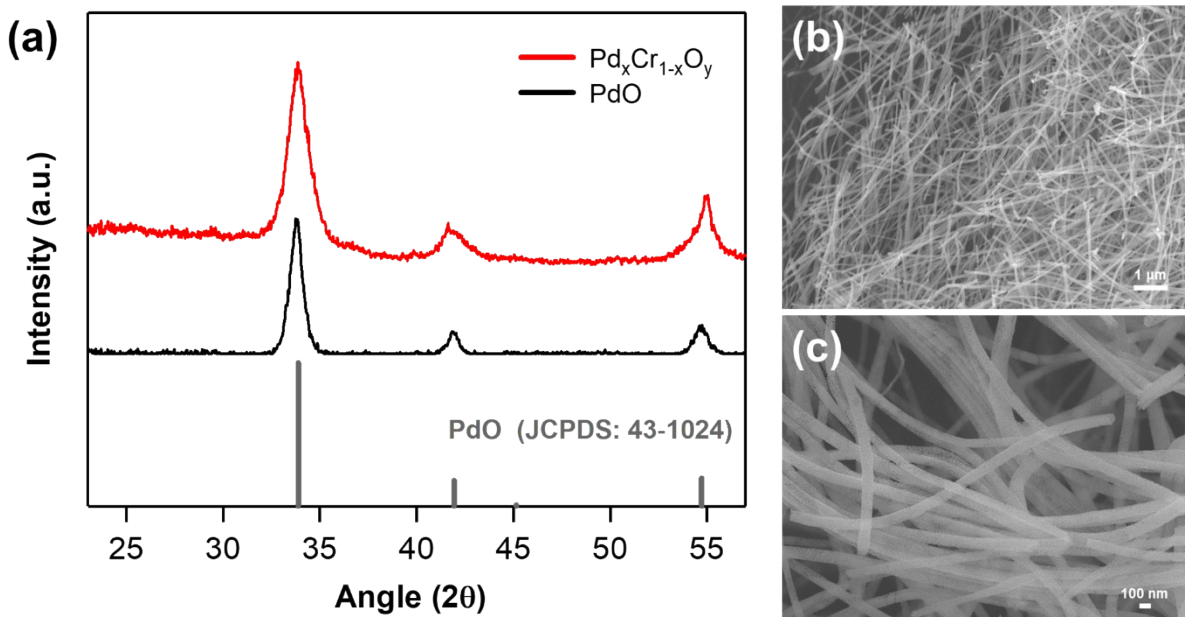

Fig. S1. (a) XRD patterns of $Pd_xCr_{1-x}O_y$ before H_2-reduction process, single PdO and reference PdO (JCPDS: 43-1024), respectively. (b and c) SEM images of $Pd_xCr_{1-x}O_y$ nanofibers.

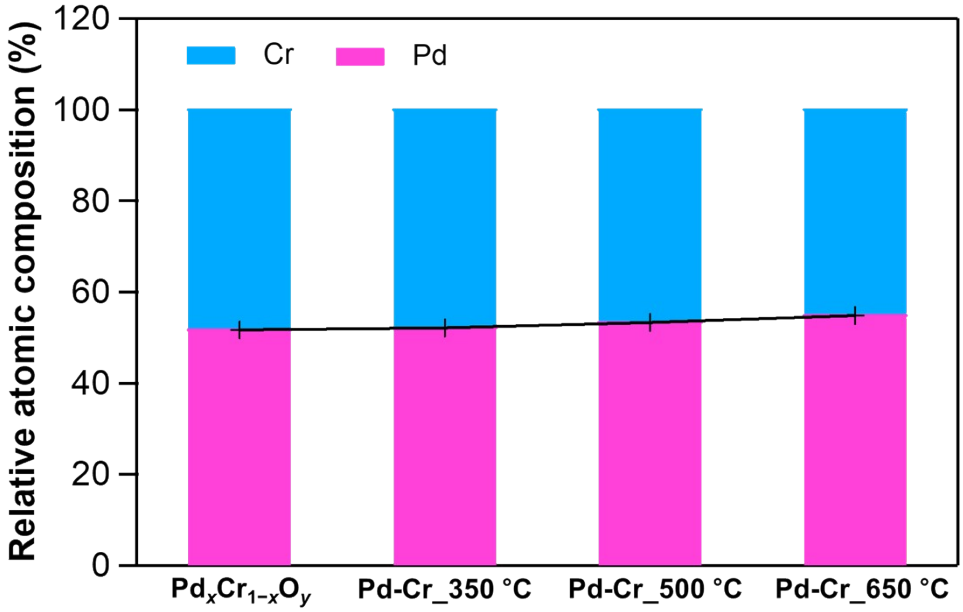

Fig. S2. Relative atomic composition ratios (Pd/Cr) of as-prepared nanomaterials.

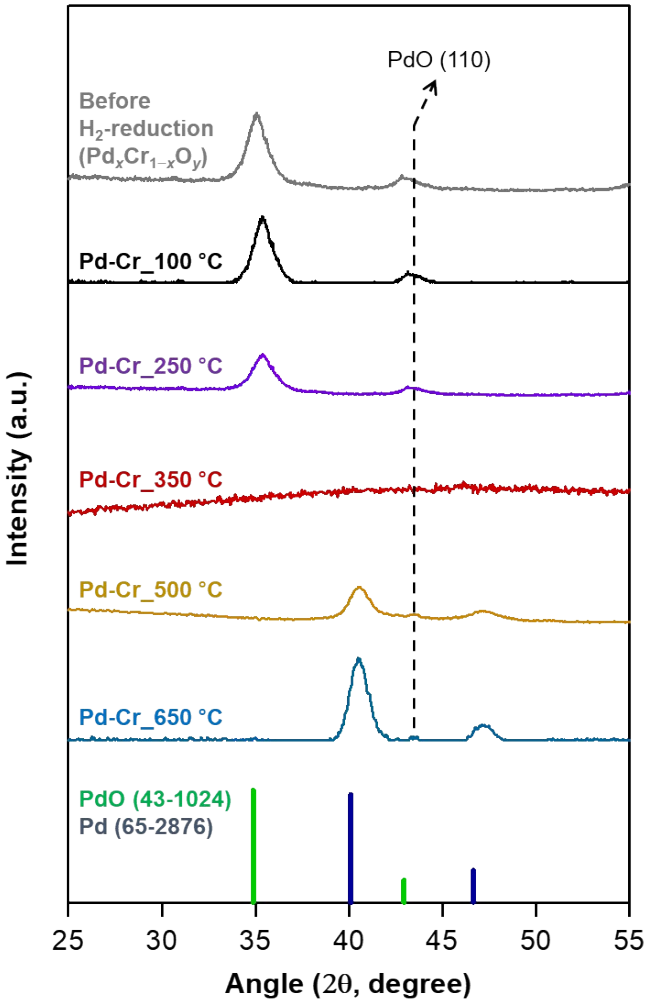

Fig. S3. XRD patterns of as-synthesized nanofibers and references (Pd for JCPDS 65-2876; PdO for JCPDS 43-1024).

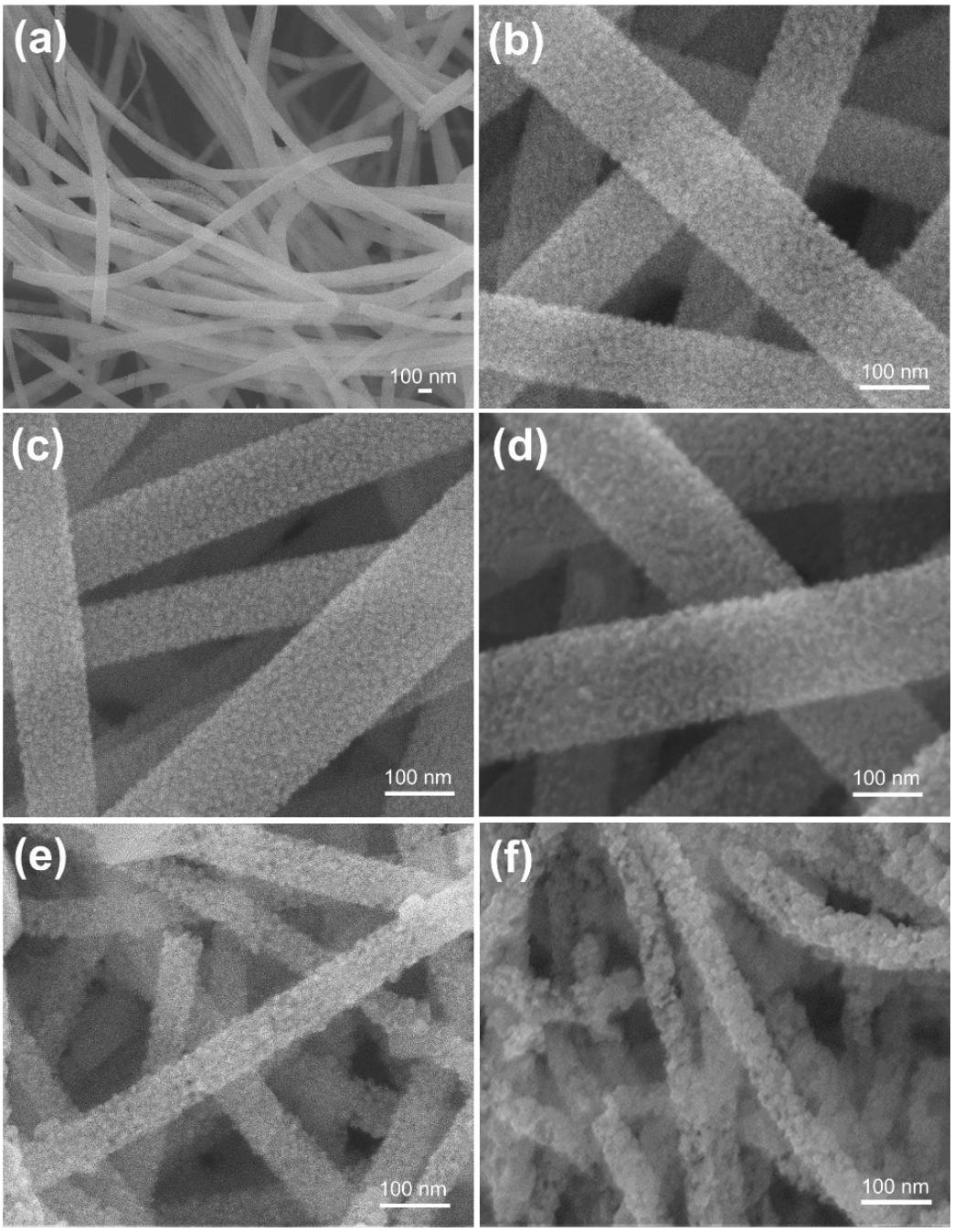

Fig. S4. SEM images of (a) $Pd_xCr_{1-x}O_y$, (b) Pd-Cr_100 °C, (c) Pd-Cr_250 °C, (d) Pd-Cr_350 °C, (e) Pd-Cr_500 °C and (f) Pd-Cr_650 °C, respectively.

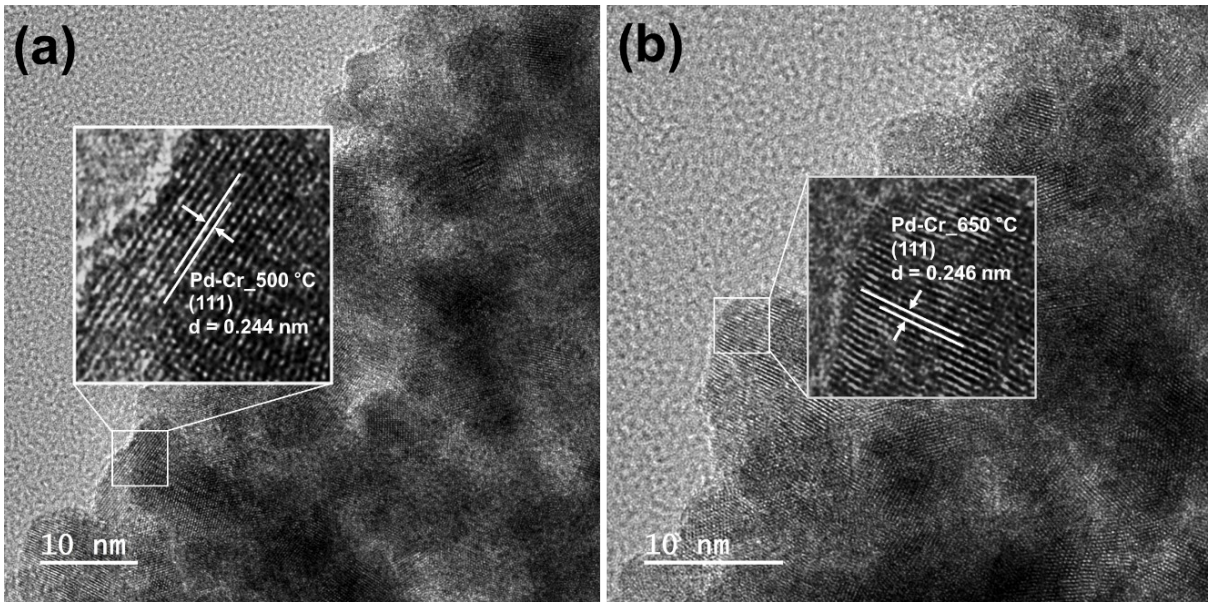

Fig. S5. HRTEM images of (a) Pd-Cr_500 °C and (b) Pd-Cr_650 °C, respectively.

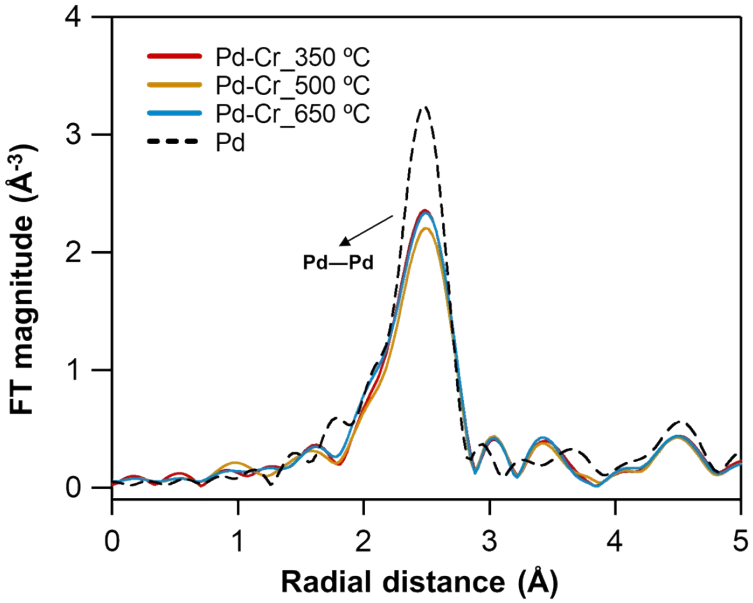

Fig. S6. Pd K-edge FT-EXAFS spectra of Pd-Cr series and reference Pd metal.

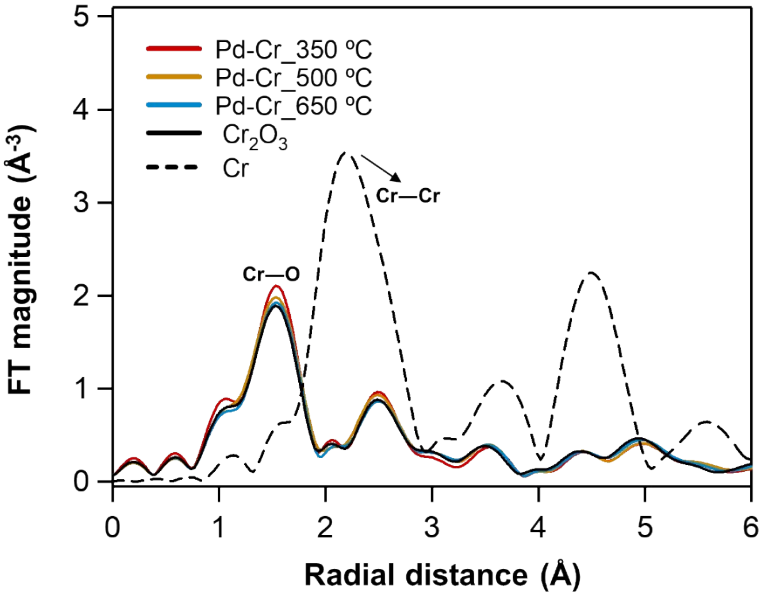

Fig. S7. Cr K-edge FT-EXAFS spectra of Pd-Cr series, Cr metal and Cr_2O_3**.**

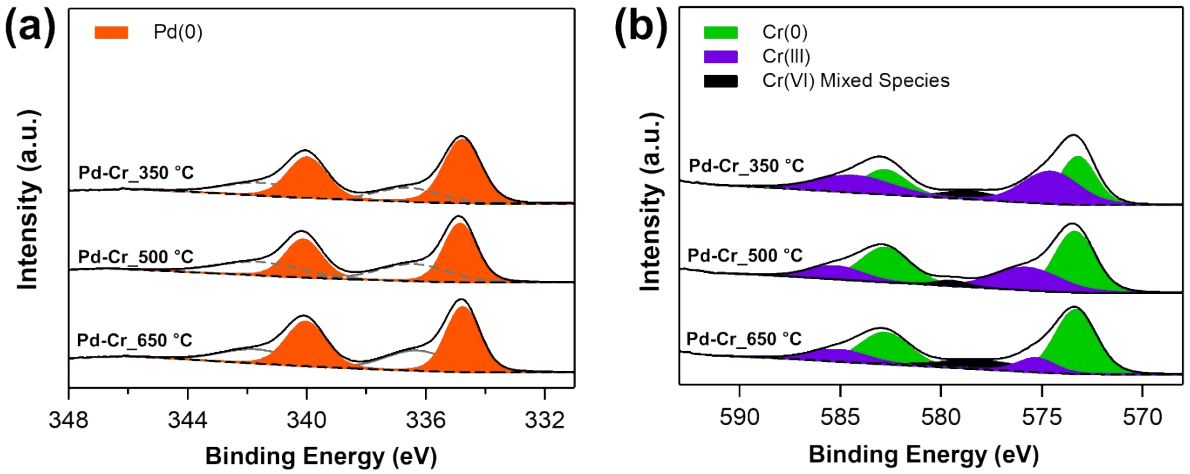

Fig. S8. XPS spectra of binary Pd-Cr samples in (a) Pd 3d region and (b) Cr 2p region at a depth of 12 nm from the surface.

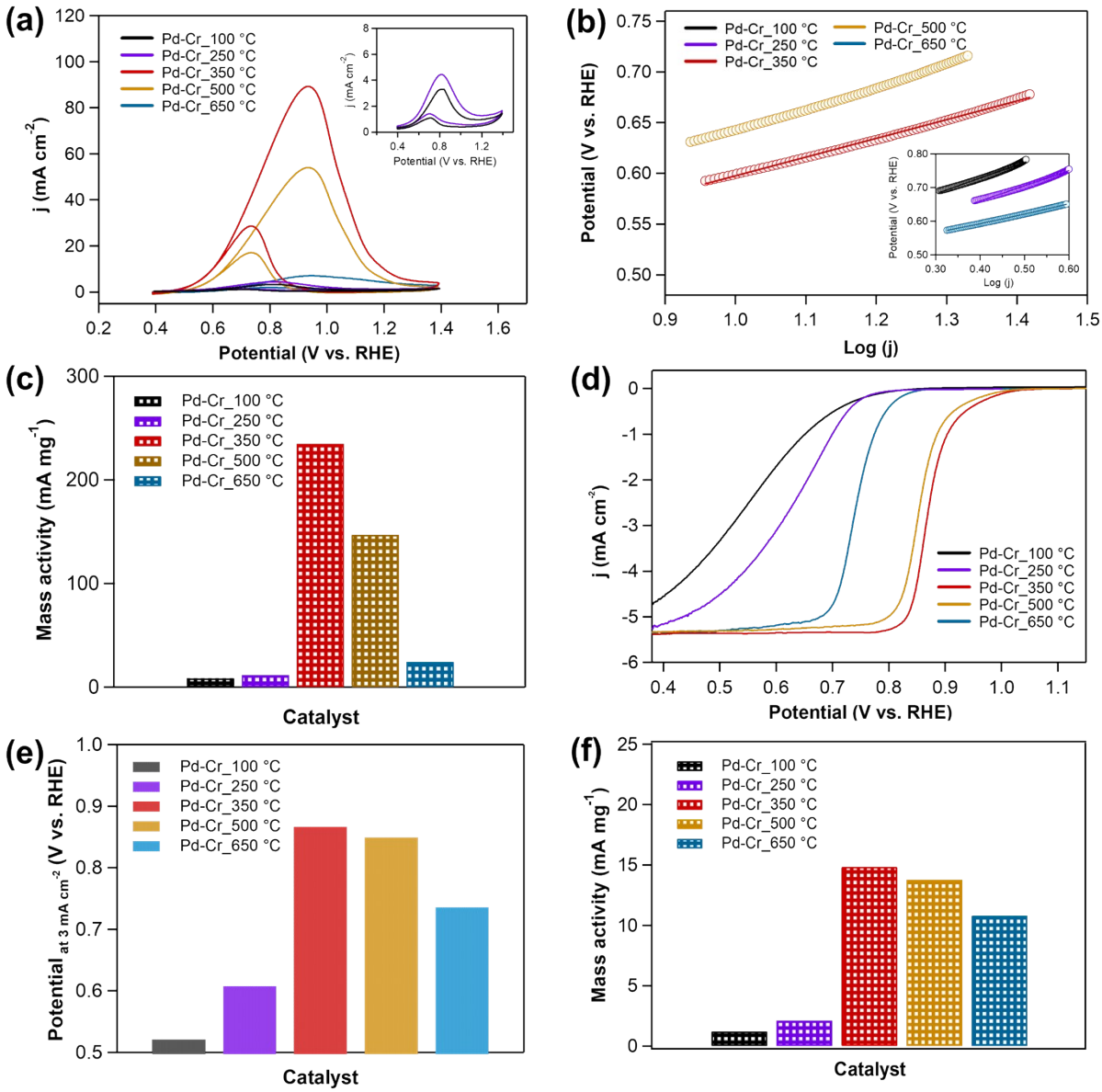

Fig. S9. Electrocatalytic (a-c) methanol oxidation reaction and (d-f) oxygen reduction reaction performances of binary Pd-Cr nanofiber series. (a) Cyclic voltammograms (CVs) of Pd-Cr series in Ar-saturated 1 M KOH solution containing 1 M CH_3OH at a scan rate of 20 mV s^{-1}. (b) Tafel plots derived from the voltammograms in (a). (c) Comparison of mass activities of as-obtained catalysts for the MOR at peak potential during forward scan. (d) ORR polarization curves of various catalysts in O_2-saturated 0.1 M KOH with a rotation rate of 1600 rpm and a scan rate of 10 mV s^{-1}. (e) Comparison of potential at 3 mA cm^{-2} from the curves in (d). (f) Comparison of mass activities of as-obtained catalysts for the ORR at 0.7 V.

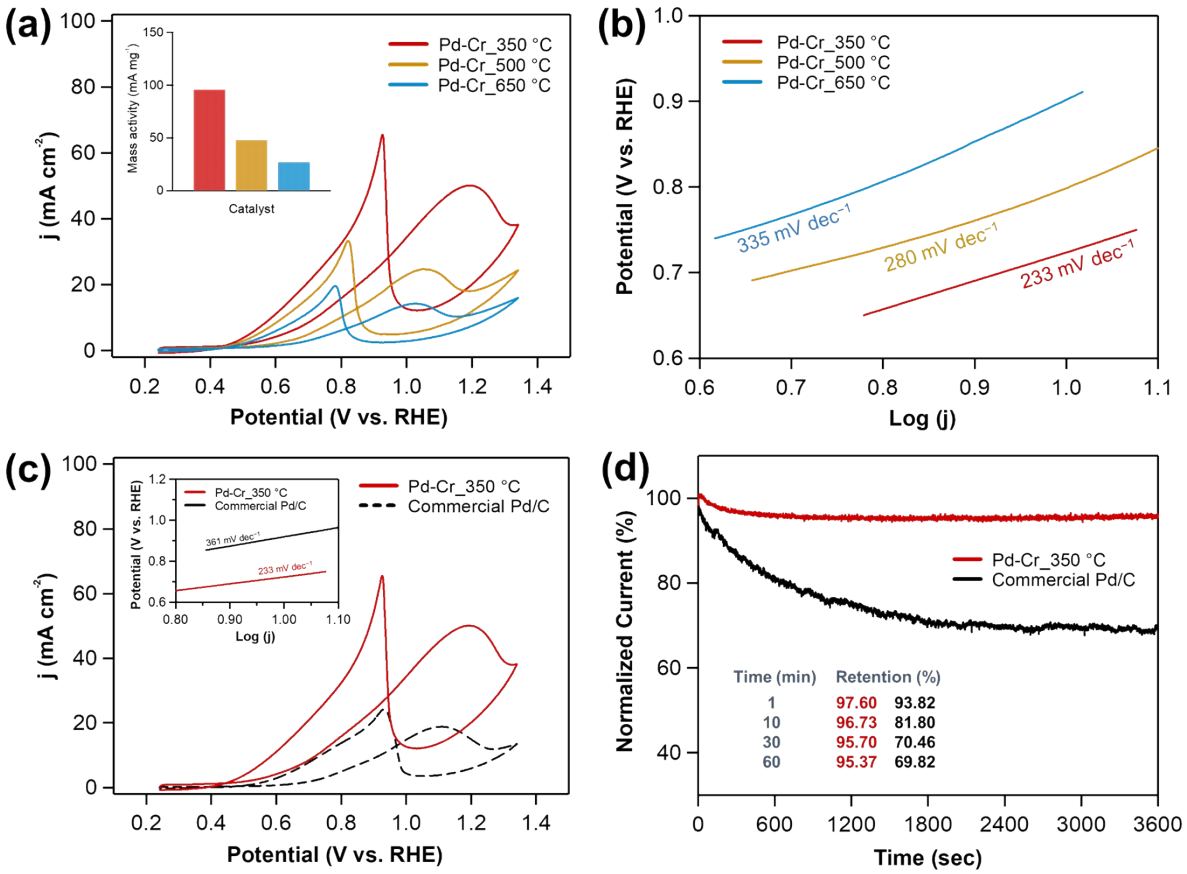

Fig. S10. Electrocatalytic MOR performances in Ar-purged 1 M $HClO_4$ solution containing 1 M methanol. (a) Cyclic voltammograms (CVs) of binary Pd-Cr nanofiber series at a scan rate of 20 mV s^{-1}. Inset: Comparison of mass activities at the peak potential during forward scan. (b) Tafel plots derived from the voltammograms in (a). (c) CVs of Pd-Cr_350 °C and commercial Pd/C toward MOR at a scan rate of 20 mV s^{-1}. Inset: corresponding Tafel plots. (d) Chronoamperometric curves with Pd-Cr_350 °C and commercial Pd/C at the respective potentials for 1 h. The respective anodic peak potentials during the forward scan were applied.

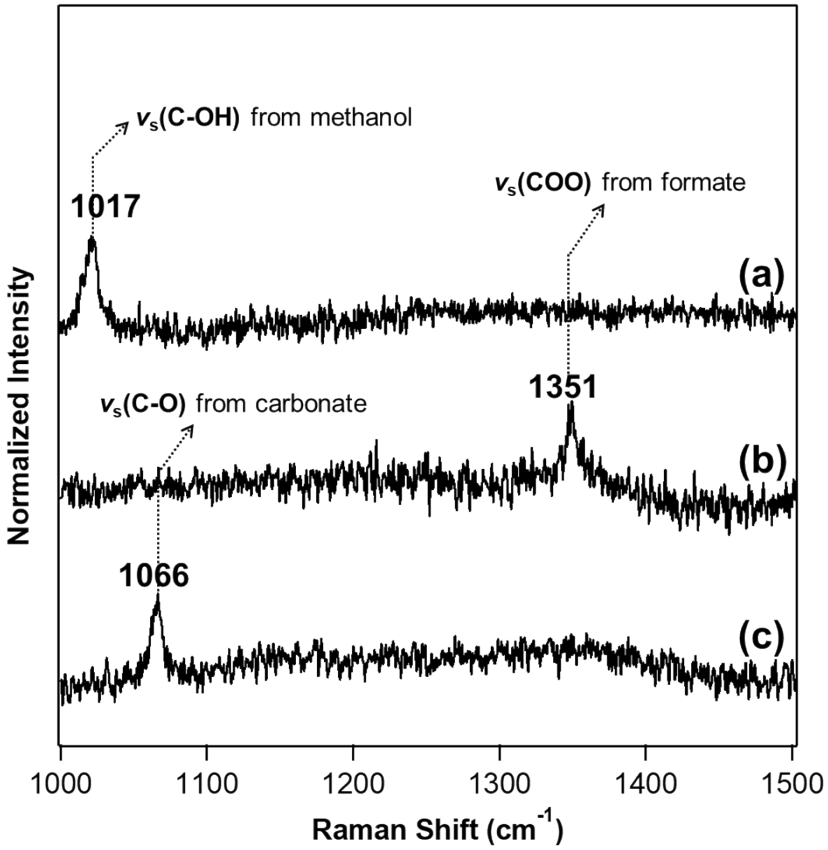

Fig. S11. Raman spectra for solutions of (a) 1 M CH_3OH in 1 M KOH, (b) 1 M HCOOH in 1 M KOH and (c) 1 M K_2CO_3 in 1 M KOH.

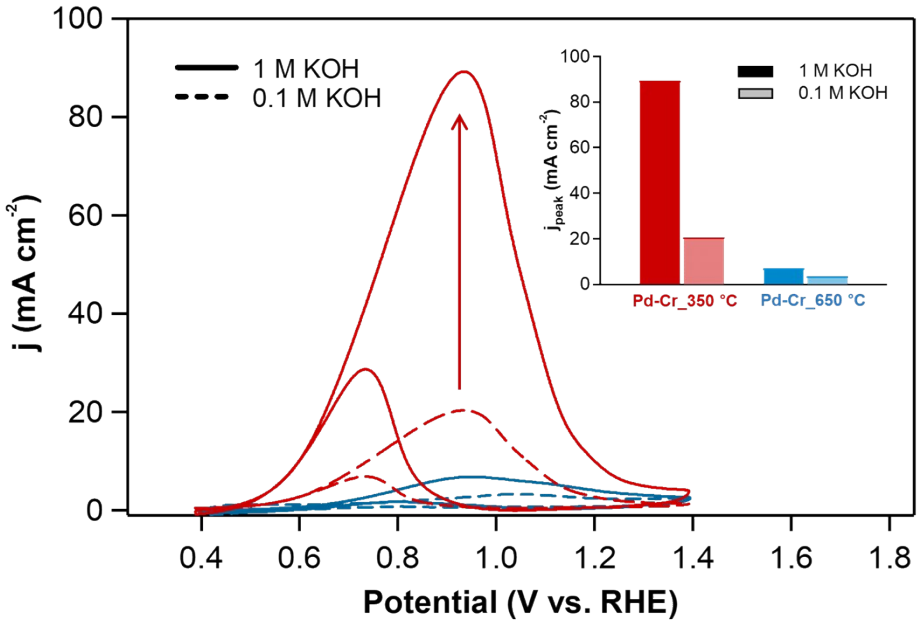

Fig. S12. CVs of Pd-Cr_350 °C (red color) and Pd-Cr_650 °C (blue color) under *x* M KOH (*x* = 0.1 and 1) containing 1 M methanol at a scan rate of 20 mV s^{-1}. The current values were normalized to the geometrical electrode surface area. Inset: Comparison of the respective peak current densities during the forward scan.

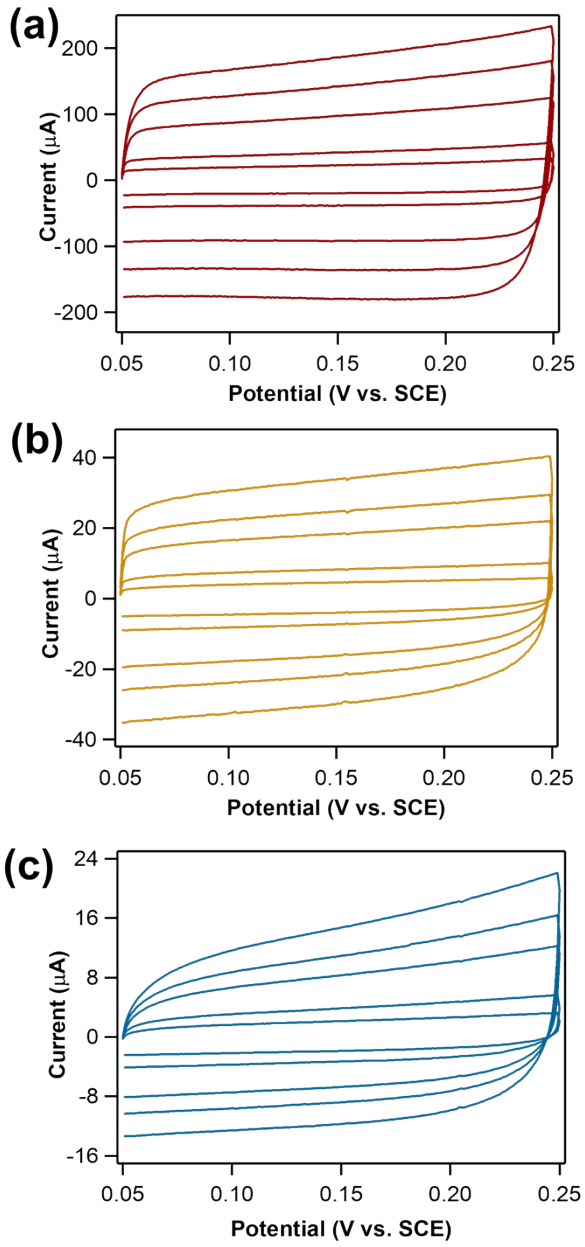

Fig. S13. CVs of (a) Pd-Cr_350 °C, (b) Pd-Cr_500 °C and Pd-Cr_650 °C in 1 M KNO_3 (*aq*) solution at various scan rates of 10, 20, 50, 70 and 100 mV s^{-1} with a potential range of 0.2 V.

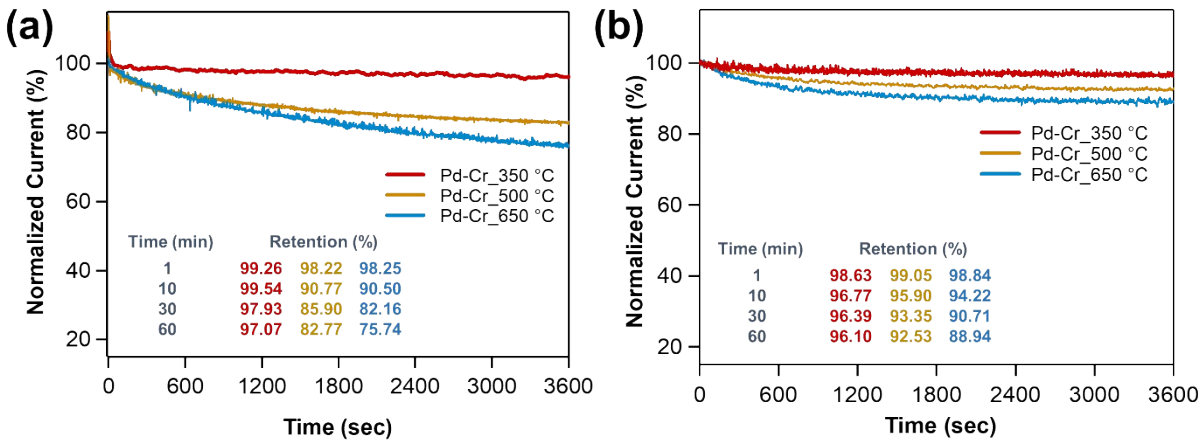

Fig. S14. Chronoamperometric measurements with various Pd-Cr nanofiber series at respective potentials for 1 h toward (a) MOR and (b) ORR. For all measurements in (a) and (b), electrochemical responses were investigated in Ar-saturated 1 M KOH solution containing 1 M CH_3OH and O_2-saturated 0.1 M KOH solution with a rotation speed of 1600 rpm, respectively.

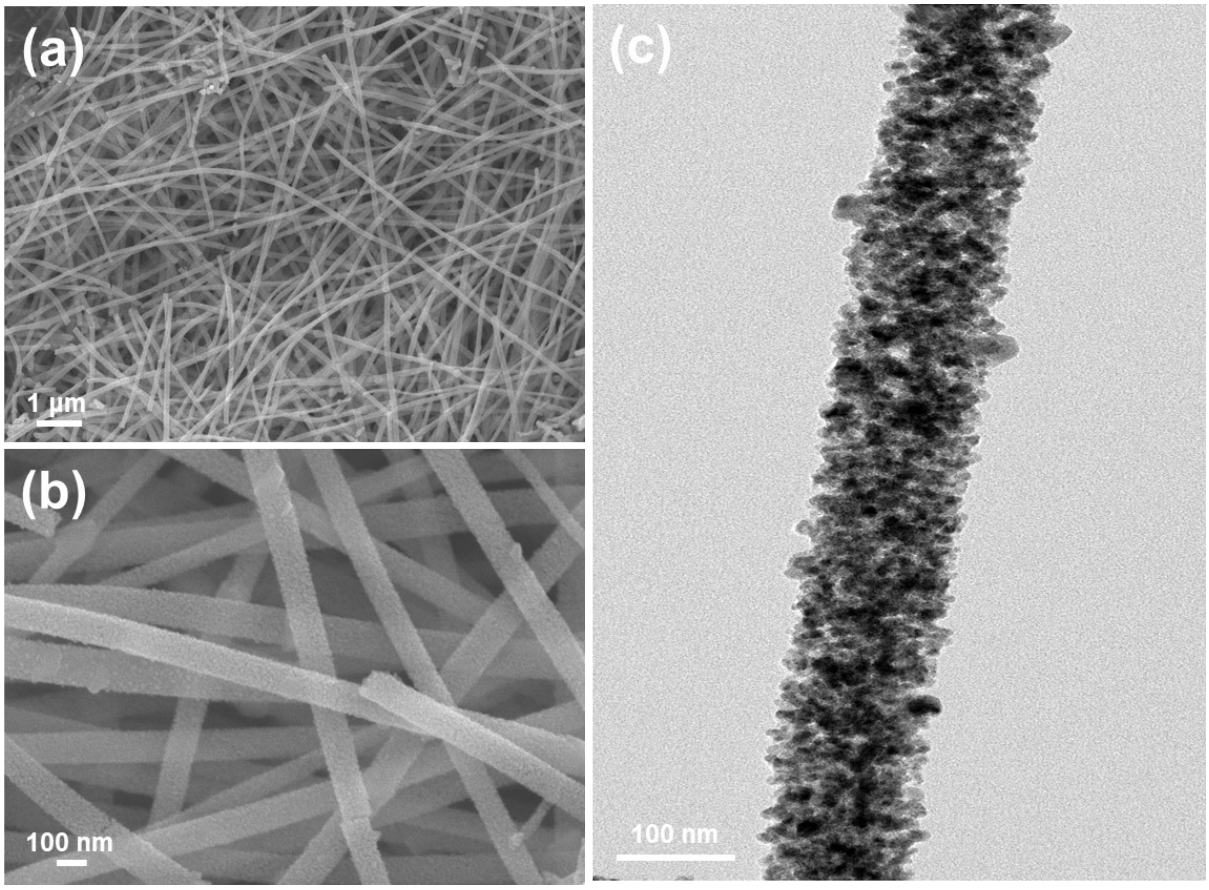

Fig. S15. (a and b) SEM images and (c) TEM image of Pd-Cr_350 °C obtained after the continuous MOR corresponding to Fig. 4(c).

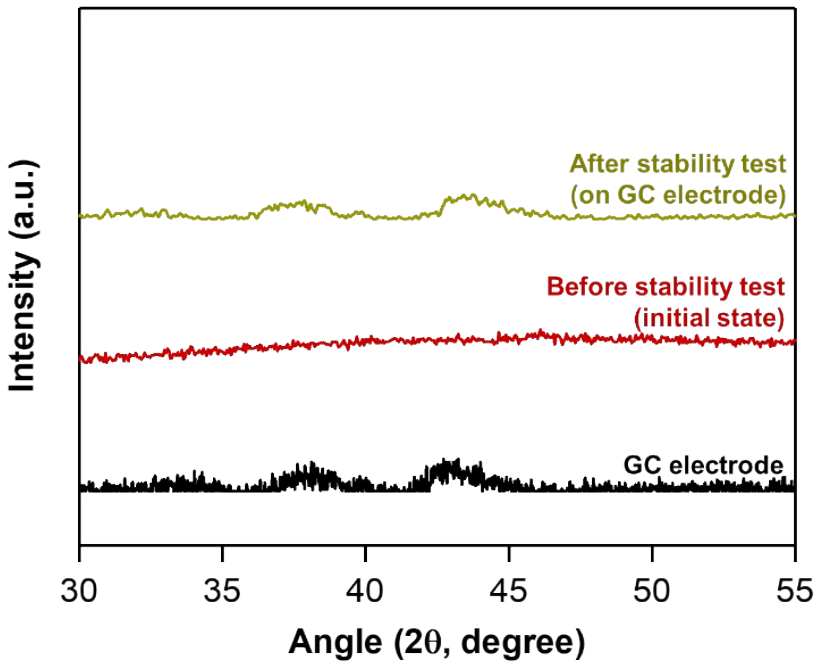

Fig. S16. XRD patterns of GC electrode (*d*=3 mm) and Pd-Cr_350 °C before (initial state) and after durability test in 1 M KOH solution containing 1 M CH_3OH. The diffraction pattern after stability test were estimated on the GC electrodes.

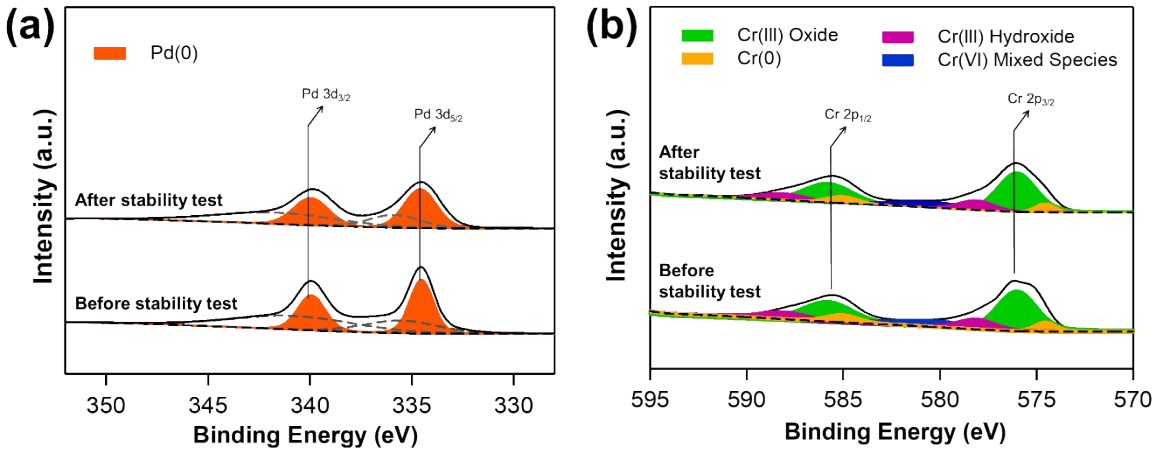

Fig. S17. XPS spectra of Pd-Cr_350 °C before (initial state) and after continuous MOR operation for 3600 s in (a) Pd 3d region and (b) Cr 2p region.

Table S1. Comparison of electrochemical properties of previously reported Pd-based bifunctional catalysts for alkaline methanol oxidation reaction and oxygen reduction reaction.

Electrocatalyst	MOR		ORR		Reference
	Mass activity	CO stripping test	Half-wave potential ($E_{1/2}$)	Stability test /Methanol tolerance test	
Pd-Cr_350 °C	235 mA mg^{-1}	−0.269 V (vs. SCE)	0.868 V (vs. RHE)	5000 cycles and chronoamperometric performances for 3600 s /Excellent tolerance	This study
PdNi/CMK-3-D(10)	300.46 A g^{-1}	0.09 V (vs. Ag/AgCl)	−0.20 V (vs. Ag/AgCl)	500 cycles /Enhanced tolerance to carbonaceous intermediates	Mater. Chem. Phys., 2020, 243, 122570
Sphere-like PdNi Alloy	518 mA mg^{-1}	-	0.854 V (vs. RHE)	-	ACS Sustainable Chem. Eng. 2023, 11, 14, 5345–5355
Ni–Pd–P@graphitic carbon	1.101 A mg^{-1}	-	0.838 V (vs. RHE)	-	Int. J. Hydrog. Energy, 2021, 46, 22499-22507
Pd_4Sn WNWs/C	1.04 A mg^{-1}	*ca*. 0.80 V (vs. RHE)	0.929 V (vs. RHE)	10 000 cycles	Nano Lett. 2019, 19, 6894–6903
Pd_2N nanocrystal	3.17 mA μg^{-1}	*ca*. 0.80 V (vs. RHE)	0.916 V (vs. RHE)	10 000 cycles	J. Mater. Chem. A, 2021, 9, 6196-6204
D-PdPtCu/C	8.82 A mg^{-1}	−0.550 V (vs. Ag/AgCl)	0.954 V (vs. RHE)	20 000 cycles /CO tolerant	Nano Lett. 2023, 23, 3467–3475

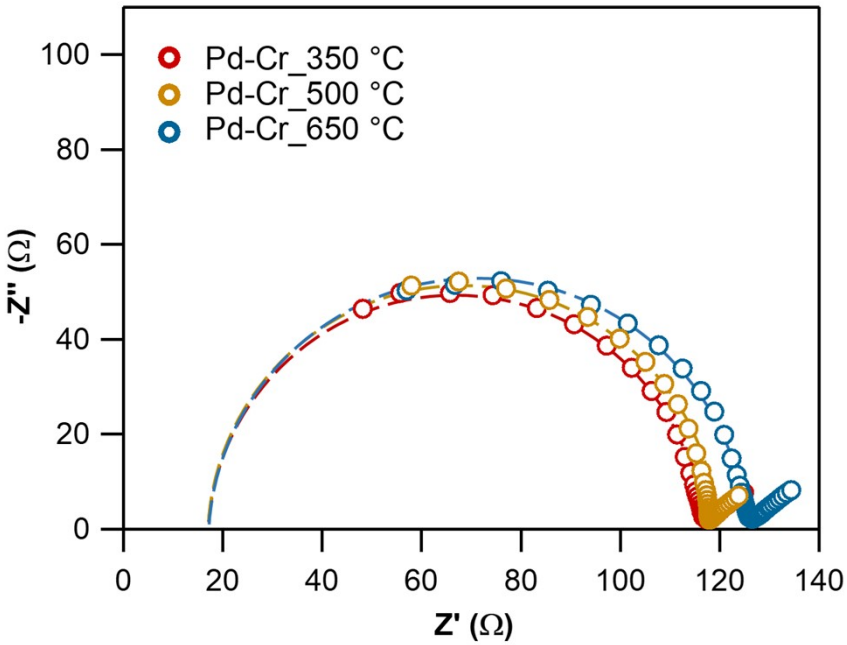

Fig. S18. Impedance spectroscopic study of binary Pd-Cr nanofiber series at 0.4 V under O_2-saturated 0.1 M KOH (*aq*).

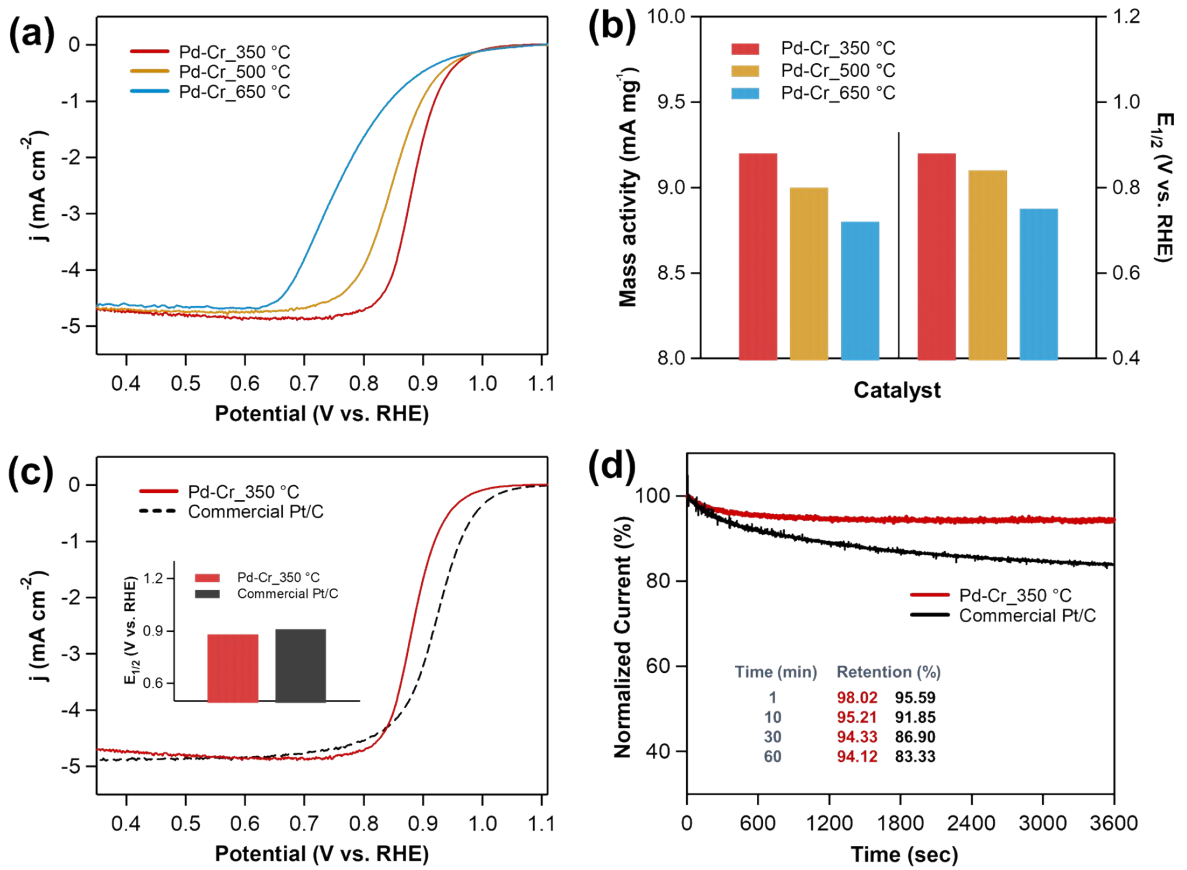

Fig. S19. Electrocatalytic ORR performances in O_2-saturated 0.1 M $HClO_4$ solution. (a) LSVs of binary Pd-Cr nanofiber series. (b) Comparison of mass activities and half-wave potentials of as-obtained catalyst for the ORR in (a). (c) LSVs of Pd-Cr_350 °C and commercial Pt/C toward ORR. Inset: corresponding half-wave potentials. (d) Chronoamperometric curves with Pd-Cr_350 °C and commercial Pt/C at 0.4 V for 1 h.

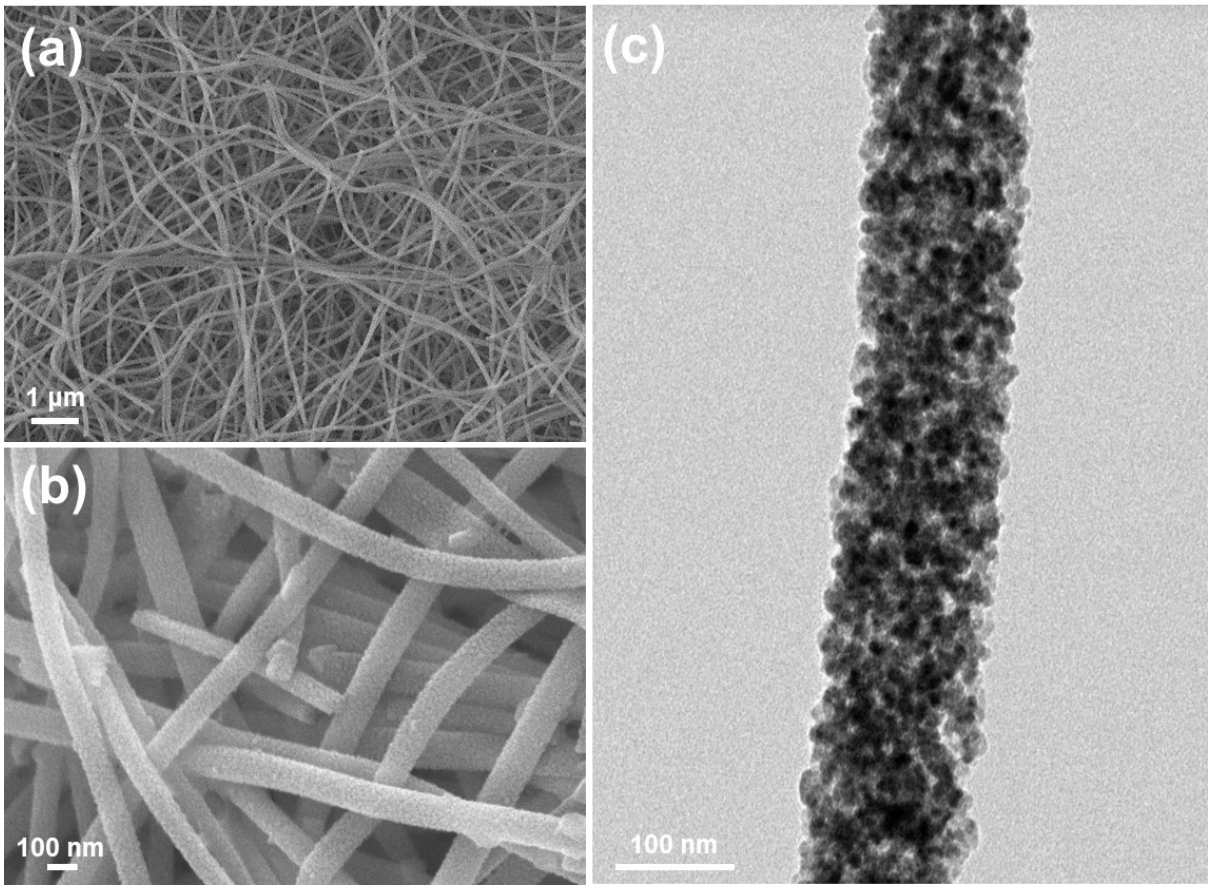

Fig. S20. (a and b) SEM images and (c) TEM image of Pd-Cr_350 °C obtained after 5000 potential cycles between 0.7 and 0.9 V (*vs*. RHE) in O_2-saturated 0.1 M KOH.

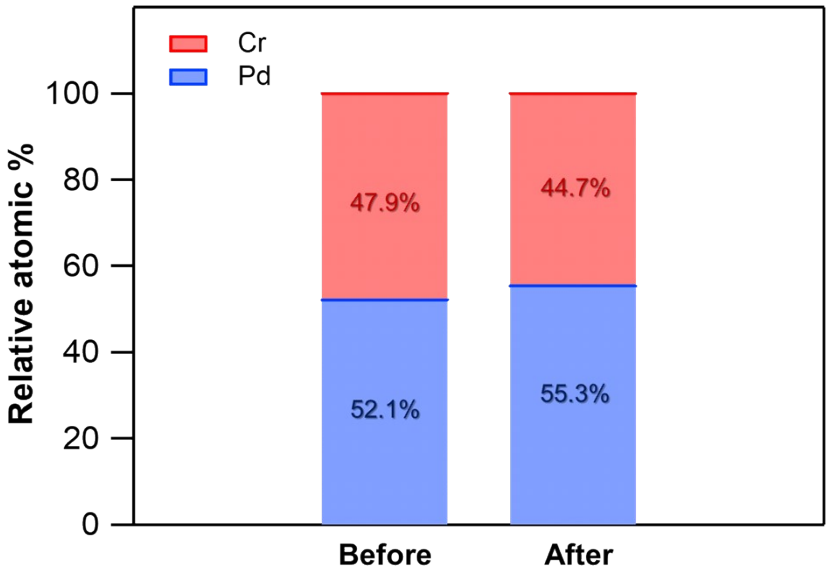

Fig. S21. Relative atomic ratio (Pd/Cr) of Pd-Cr_350 °C nanofibers before and after the stability test in Fig. 6(b). The element in percentage was calculated from the EDS measurements, and the EDS spectra were collected from the different 15 spots.